MRI Motion Artefacts Introduction and Correction using Complex-Valued Artificial Fourier Transform (AFT)-Net

BMEN4460 Deep Learning in Biomedical Imaging - Final Report

Quentin Chappat
Department of Biomedical Engineering
Columbia University in the City of New York
New York City, USA
qjc2002@columbia.edu

Nikhil Kuppa
Department of Biomedical Engineering
Columbia University in the City of New York
New York City, USA
nkk2126@columbia.edu

Zachary Abassera
Department of Biomedical Engineering
Columbia University in the City of New York
New York City, USA
zca2001@columbia.edu

***Abstract*— MRI is very sensitive to motion, and thus motion related artefacts are a very common sight. Motion during scans degrades the image quality to the extent that patients may need to be called back for a repetition of the scan. This causes a lot of inconvenience to both the patient as well as the hospitals, and a lot of time is consumed. In this paper, we introduce motion artifacts, test the proposed novel complex-valued deep learning framework of Artificial Fourier Transform Network (AFT-Net), and discuss how well it corrects these motion artifacts during the image reconstruction task.**

Keywords*— *MRI reconstruction, motion artifacts, motion correction, biomedical imaging, Fourier transform.

I. Introduction

Magnetic resonance imaging is a modality that uses magnetic fields and computer-generated radio waves to generate detailed images of organs and tissues in the body. The MRI machines are long tube-shaped magnets in which the role of the magnetic field is to temporarily realign water molecules in the body so that the radio waves can cause these aligned atoms to produce faint signals in order to create cross-sectional MRI images — like slices in a loaf of bread. [1]

The organ being imaged in the machine is encoded using a strong magnet, radiofrequency (RF) pulses, and gradients, and the signal generated is digitized using an Analog to Digital Converter. This data is arranged in a complex array known as k-space, and has phase and frequency encoded data along the y-axis and x-axis respectively. K-space data is then decoded to generate an image through reconstruction techniques. [2]

Currently, Discrete Fourier Transform (DFT) is used as a common technique for transforming this frequency domain k-space data to the image domain. The issue however is that DFT is known to introduce a lot of artifacts like the Gibbs effect around the edges. The distortion caused by reconstruction cannot be restored from conventional imaging processing methods due to information loss inevitably caused during the domain conversion.

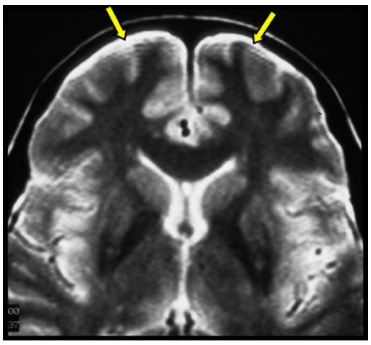

Fig 1. Gibbs Ringing Artifact due to Fourier Transform

To solve the problem mentioned above, Yanting Et. al. propose a unified complex-valued image reconstruction approach for magnetic resonance images, which aims to remove any non- deep learning method in the workflow and incorporate data processing into deep learning frameworks [3]. The framework they describe in the study is the artificial Fourier transformation (AFT) which has the full functionality of a state-of- the-art Fourier transform. They utilize AFT combined with deep complex networks, U-Net specifically, to design the artificial Fourier transform network (AFT-Net) for MRI reconstruction and denoising. Given raw k-space data with a low signal-to-noise ratio (SNR), AFT-Net is proven to

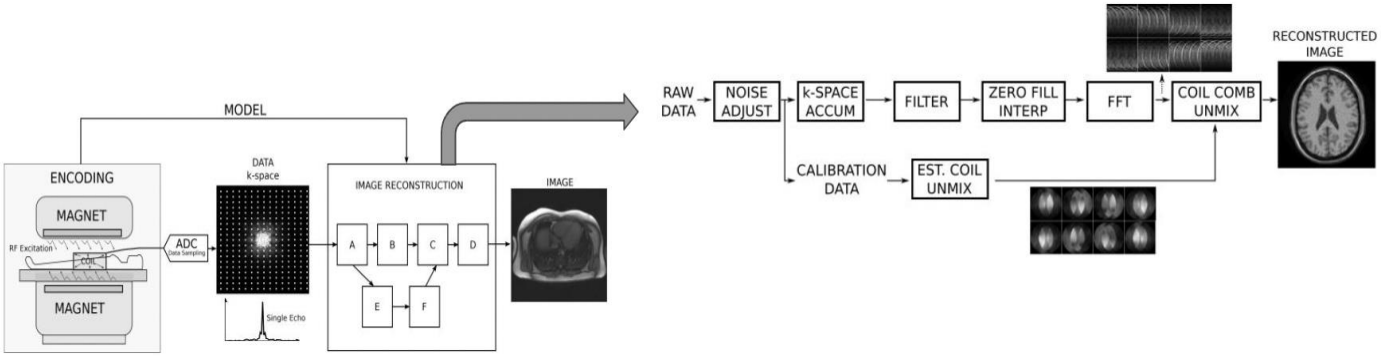

Fig 2. MRI Image Acquisition Process [2]

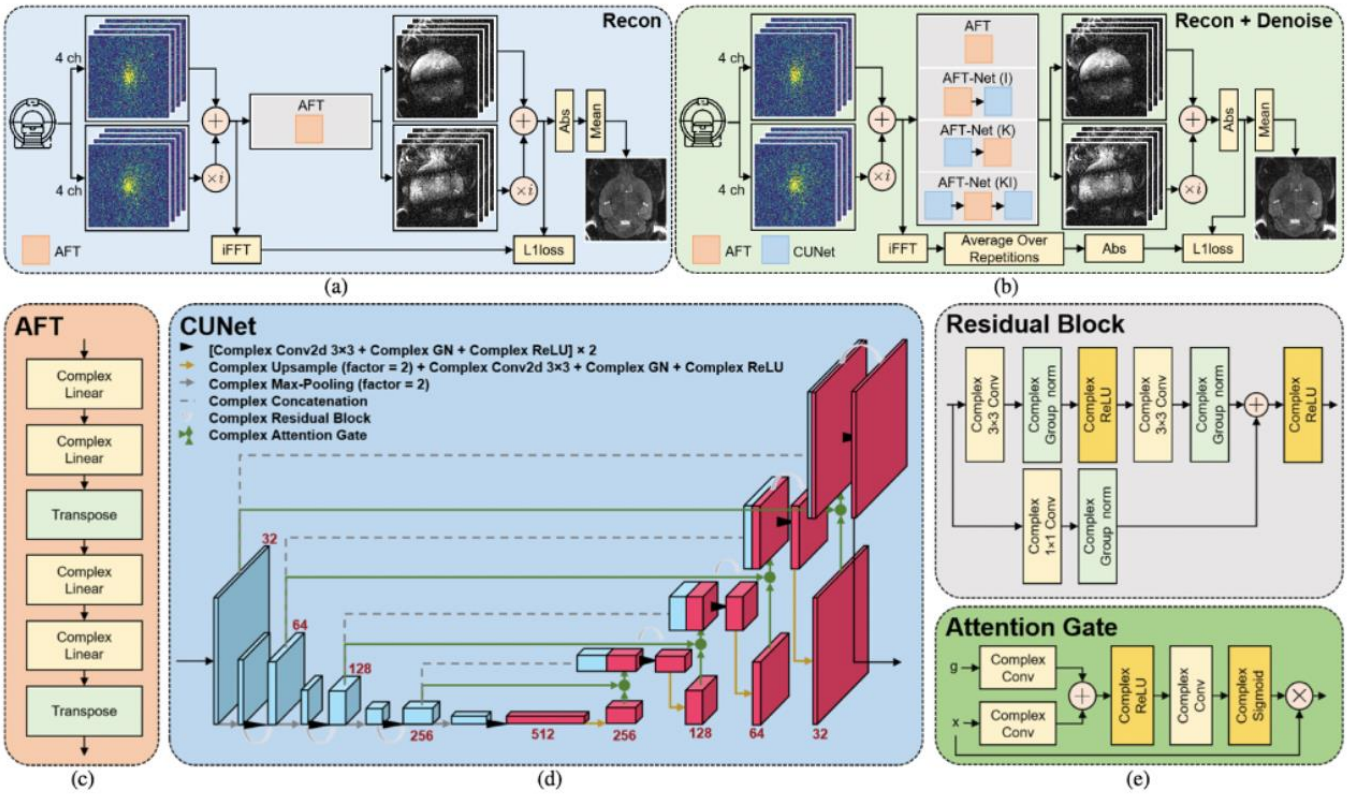

Fig 3. Overview of the AFT-Net framework. (a) Workflow for the reconstruction task. The target is derived by taking iFFT over the raw k-space data, and AFT is evaluated over this task. (b) Workflow for the reconstruction plus denoising task. The target is derived by taking the average over repetitions after iFFT. (c) Structural of the AFT with two successive blocks, which consist of two complex linear layers followed by a transpose operation. (d) Structural of the CUNet, a complex version of residual attention U-Net with all the real-valued components replaced by complex-valued components. (e) Structural of the complex residual block and the complex attention gate.

learn the mapping between two domains and remove noise while preserving useful structural information.

Motion artifacts are very common and can negatively affect any diagnosis. The k-space data is sampled along the frequency-encoded axis almost instantaneously, unlike the phase-encoded axis sampling, which occurs in the magnitude of seconds or minutes because all lines of k-space must be collected to get the entire set needed for Fourier Reconstruction.

Most physiological motions like respiration, swallowing and cardiac pulsation take between 100ms to several seconds, and are slower relative to the frequency-encoded sampling interval. Thus there is a very minute amount of spatial blurring locally in this axis. However, since the phase sampling interval is equal or longer than most motions, motion artifacts are significant in this direction [4]. In this project, we attempt to introduce subtle motion artifacts into the dataset and test the AFT-Net and related models on their ability to reconstruct the target image.

II. Algorithms Implemented [3]

A. *Artificial Fourier Transform - AFT*

AFT is Artificial Fourier Transform which specializes in the task of image reconstruction from k-space to image domain. It is a complex-valued neural network that is based on the 2D DFT.

B. *Artificial Fourier Transform Network – AFT-Net*

AFT-Net is a combination of the AFT algorithm and the CU-Net algorithm – which is a complex valued version of the popular convolutional neural network algorithm that is widely used for biomedical image segmentation tasks – U-Net. The AFT-Net comes in three different types, and they are as follows:

1) AFT-Net (I)

AFT-Net (I) is an algorithm in which the output of the AFT is fed to the input of the CU-Net in order to perform the reconstruction task.

2) AFT-Net (K)

AFT-Net (K) is an algorithm in which the output of the CU-Net is fed to the input of the AFT in order to perform the reconstruction task along with denoising. The idea is that the CU-Net extracts relevant significant features from the k-space and only these raw k-space domain features are used for the reconstruction task to the image domain – thus also performing denoising in the process.

3) AFT-Net (KI)

AFT-Net (KI) is an algorithm in which the output of the CU-Net is fed to the input of the AFT, and its output is fed into the CU-Net again in order to perform the reconstruction task along with accelerated imaging. In this algorithm the first CU-Net extracts relevant significant features from the k-space and the second CU-Net extracts relevant features from the image domain.

III. Dataset Used

For this project, we are using NYU Langone's fastMRI dataset which is a publicly available dataset of raw k-space data corresponding fully sampled MRI images. This dataset was created by researchers at New York University and Facebook AI Research in collaboration and contains knee and brain MRI scans. It includes axial T1-weighted, T2-weighted and FLAIR images scanned with 4 coils and magnetic field strengths of 3T and 1.5T.

While the dataset contains 6970 fully sampled brain MRI scans, we are focusing only on a subset of the brain data part of this dataset, and we'll be using 801 fully sampled brain MRIs obtained on 3 and 1.5 Tesla magnets. This subset has 692 T2 weighted scans obtained using 1.5 Tesla magnets, and 109 T1 weighted scans obtained using 3 Tesla magnets.

IV. Methods

To apply AFT-Net for motion correction, our approach was two-fold:

A) Create a motion-corrupted dataset using the Brain MRI data.

B) Test AFT-Net's different configurations upon training T1-weighted scans and T2-weighted scans individually, and together.

To introduce motion artifacts into the images, we attempted using the TorchIO package. However, the issue with this package was that there was a significant amount of phase information loss as the package considered only the absolute values of the complex image as its input, and not the complex image itself. We then modified the class 'RandomMotion' in this package such that motion transformations are applied to the real and imaginary parts individually and then combined to get the complex motion corrupted image. It is from this motion corrupted image that the motion corrupted k-space is generated.

We then augmented our data by 2 times, by creating a simulated-corrupted-k-space for each raw-uncorrupted-k-space using this modified version of the package TorchIO and used this augmented dataset as the training data for our model. We made sure to keep our two classes (corrupted and uncorrupted) balanced in each of our fold (60% training, 20% validation, and 20% testing). All fifteen of our models (AFT, CU-Net, AFT-Net (I), AFT-Net (K), and AFT-Net (KI) models each for T1 and T2 individually and then combined) were trained using the Google Colaboratory Virtual Machines with NVIDIA A100 GPUs (12 GB VRAM). Having let all our models train until the end, the total cumulated training time came to be about 180 hours.

AFT and CU-Net were pretrained individually and then used in the transfer learning for the AFT-Net models. The optimizer used was Adam with a decaying learning rate, the loss function used was the mean squared error between the reconstructed motion-free image and the reconstructed motion-corrupted image. The validation score used was the Structural Similarity Index Measure (SSIM).

V. Results

The following are the visual results of the models trained on T1 and T2 datasets individually as well as trained together.

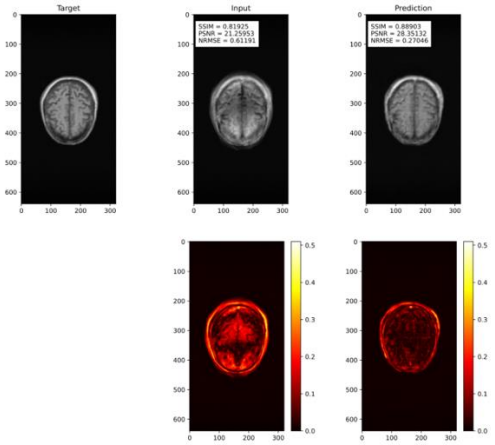

Fig 4. Motion Correction with AFT-Net (KI) trained on T1

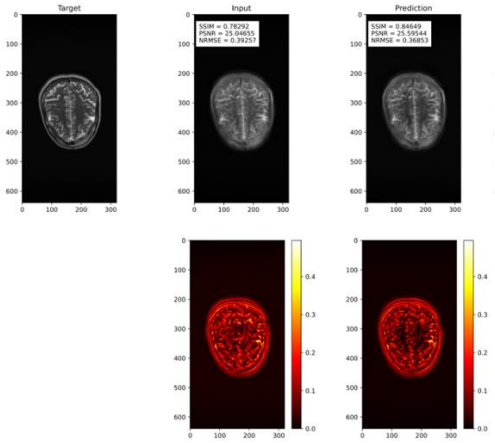

Fig 5. Motion Correction with AFT-Net (K) trained on T2

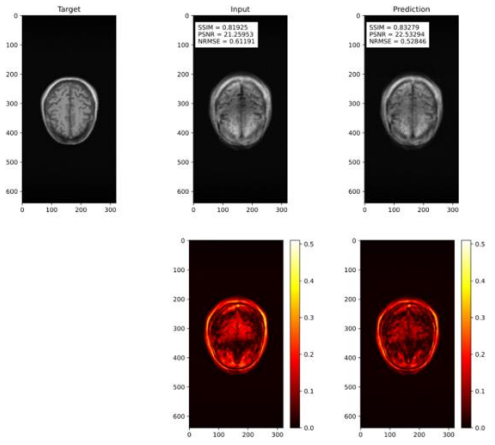

Fig 6. T1 image motion correction with AFT-Net (K) trained on both

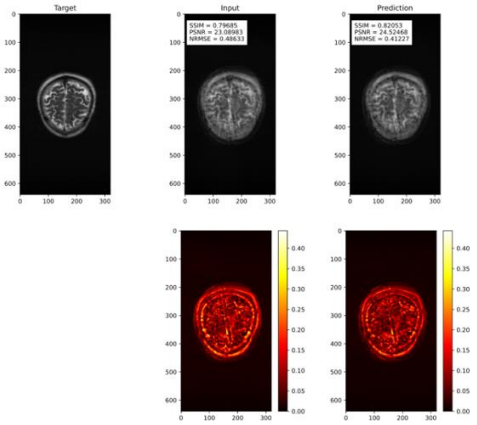

Fig 7. T2 image motion correction with AFT-Net (K) trained on both

We observe that the AFT-Net models can reconstruct the image adequately. In particular, corrupted images' outputs have a distribution of quality metrics significantly different from their inputs (Supplemental material).

VI. Discussion

We managed to develop a pipeline to simulate motion artefacts on raw k-space MRI scans without losing any information by keeping both phase & magnitude parts using a modified version of the TorchIO package. We also trained the AFT-Net on different datasets and with different configurations, and the CU-Net and AFT-Net learn features to correct motion artefacts. The improvements and the interesting aspects of our project are that we take the raw-k-space as input, which means there is no preprocessing needed, no detection of movement needed and also there is no loss of data involved - like phase.

To validate this hypothesis, our future work would include to test the current architecture on motions obtained only in a 2D space. One limitation of our models is that they are in 2D, and therefore, have a hard time correcting 3D type of motion. Modifying this network to handle raw 3D MRI data and creating a 3D AFT-Net could help correct many more artefacts.

Acknowledgment

We thank Dr Jia Guo and Dr Andrew Laine for giving us this exciting project through which we gained a lot of new skills and understood the entire deep learning based biomedical imaging workflow. We would also like to heartily thank Yanting Yang for providing us with the codes for his AFT-Net algorithm, as well as for providing us with the dataset. We would also like to thank our TAs Xuzhe Zhang and Sravan Ravi for guiding us well throughout the semester and helping us understand tough concepts with ease.

Contributions

Everyone participated in the conceptual discussions.

Quentin Chappat handled the coding of the simulation of the motion artefacts in the k-space, the training of the models, the evaluations, and the plots.

Zachary Abessera handled the creation of the slides and the scripts.

Nikhil Kuppa wrote the paper.

Everyone participated in the recording.

References

[1] Bae, J.B., Lee, S., Jung, W. *et al.* Identification of Alzheimer's disease using a convolutional neural network model based on T1-weighted magnetic resonance imaging. *Sci Rep* 10, 22252 (2020).

[2] Hansen MS, Kellman P. Image reconstruction: an overview for clinicians. J Magn Reson Imaging. 2015 Mar;41(3):573-85.

[3] Y. Yang, J, Guo, A. Laine, "Deep Learning-based MRI Reconstruction with Artificial Fourier Transform (AFT)-Net", unpublished.

[4] Wald L. MR image encoding. (From MIT OpenCourseWare http://ocw.mit.edu)

TABLE I: RESULTS ON MOTION FREE K-SPACE DATA

Dataset	T1 3T			T2 1.5T			T1 3T & T2 1.5T		
Model	SSIM	PSNR	RMSE	SSIM	PSNR	RMSE	SSIM	PSNR	RMSE
CUNet	**9.2102e-01 ± 1.1777e-02**	**3.2554e+01 ± 1.4513e+00**	**1.6120e-01 ± 4.0768e-02**	**9.8498e-01 ± 5.5918e-03**	**4.3027e+01 ± 1.4326e+00**	**5.5564e-02 ± 1.4856e-02**	**9.8000e-01 ± 7.5182e-03**	**4.1529e+01 ± 1.4636e+00**	**6.4316e-02 ± 1.4561e-02**
I	**9.8265e-01 ± 3.7489e-03**	**3.9668e+01 ± 1.3652e+00**	**7.0586e-02 ± 1.4042e-02**	**9.7115e-01 ± 1.6481e-02**	**4.0101e+01 ± 1.5884e+00**	**7.8075e-02 ± 2.8748e-02**	**9.4207e-01 ± 1.4011e-02**	**3.6691e+01 ± 1.8129e+00**	**1.1186e-01 ± 2.3939e-02**
K	**9.2710e-01 ± 1.1893e-02**	**3.2969e+01 ± 1.9409e+00**	**1.5702e-01 ± 6.0112e-02**	**9.4638e-01 ± 2.1725e-02**	**3.7201e+01 ± 1.7370e+00**	**1.0886e-01 ± 3.7124e-02**	**9.6380e-01 ± 1.6273e-02**	**3.9053e+01 ± 1.4115e+00**	**8.5600e-02 ± 2.5653e-02**
KI	**9.0636e-01 ± 1.6601e-02**	**3.0627e+01 ± 2.0885e+00**	**2.0840e-01 ± 8.8545e-02**	**9.6601e-01 ± 1.7412e-02**	**3.9629e+01 ± 1.3494e+00**	**8.2621e-02 ± 3.2927e-02**	**9.5417e-01 ± 2.4976e-02**	**3.7166e+01 ± 1.9469e+00**	**1.0789e-01 ± 4.4907e-02**

TABLE II: RESULTS ON MOTION CORRUPTED K-SPACE DATA

Dataset	T1 3T			T2 1.5T			T1 3T & T2 1.5T		
Model	SSIM	PSNR	RMSE	SSIM	PSNR	RMSE	SSIM	PSNR	RMSE
Input	**8.1877e-01 ± 4.5789e-02**	**2.5598e+01 ± 3.1054e+00**	**3.6372e-01 ± 1.3294e-01**	**8.2667e-01 ± 4.2110e-02**	**2.6137e+01 ± 2.1018e+00**	**3.9201e-01 ± 1.1345e-01**	**8.2555e-01 ± 4.2741e-02**	**2.6060e+01 ± 2.2793e+00**	**3.8799e-01 ± 1.1684e-01**
CUNet	**8.7497e-01 ± 2.9343e-02**	**2.8005e+01 ± 1.9073e+00**	**2.6742e-01 ± 6.8117e-02**	**8.7046e-01 ± 3.1495e-02**	**2.7524e+01 ± 1.6587e+00**	**3.2917e-01 ± 7.5382e-02**	**8.5868e-01 ± 3.7086e-02**	**2.6921e+01 ± 2.0702e+00**	**3.4798e-01 ± 9.3188e-02**
I	**8.5325e-01 ± 4.0229e-02**	**2.7158e+01 ± 2.1591e+00**	**2.9367e-01 ± 6.8050e-02**	**8.8594e-01 ± 2.9389e-02**	**2.8198e+01 ± 1.6451e+00**	**3.0514e-01 ± 7.4697e-02**	**8.8092e-01 ± 2.8516e-02**	**2.7777e+01 ± 1.7843e+00**	**3.1275e-01 ± 7.2002e-02**
K	**8.7811e-01 ± 2.7894e-02**	**2.8252e+01 ± 1.8768e+00**	**2.6011e-01 ± 6.7219e-02**	**8.8319e-01 ± 2.7804e-02**	**2.7924e+01 ± 1.6639e+00**	**3.1422e-01 ± 7.1508e-02**	**8.6276e-01 ± 3.2724e-02**	**2.6586e+01 ± 2.0493e+00**	**3.6230e-01 ± 9.8917e-02**
KI	**8.4066e-01 ± 3.0982e-02**	**2.5598e+01 ± 2.1375e+00**	**3.5552e-01 ± 1.0082e-01**	**8.6564e-01 ± 3.0226e-02**	**2.6650e+01 ± 1.8889e+00**	**3.6720e-01 ± 9.7826e-02**	**8.7745e-01 ± 3.0659e-02**	**2.7587e+01 ± 1.8198e+00**	**3.2002e-01 ± 7.5657e-02**

Metric distributions: Mix T1 3T T2 15T Corrupted

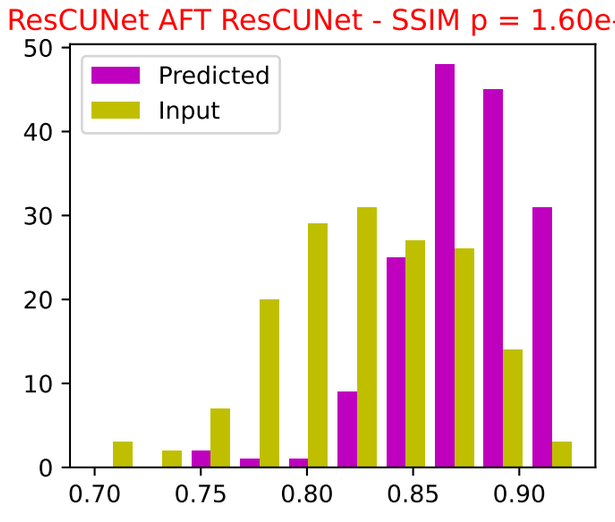

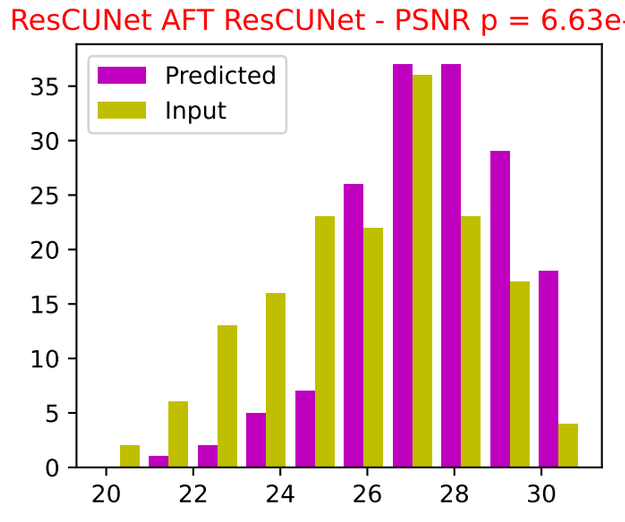

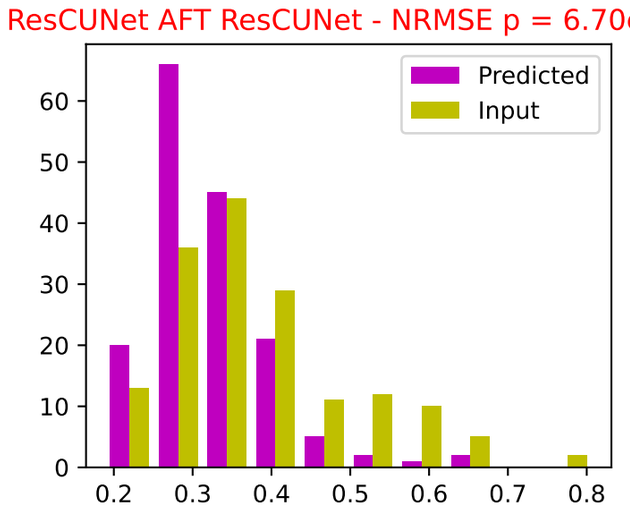

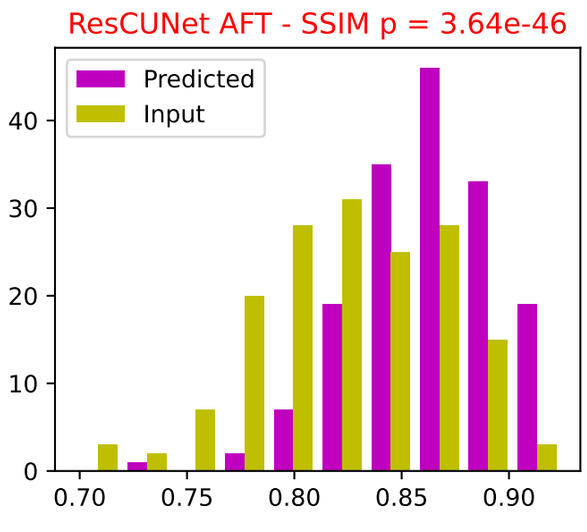

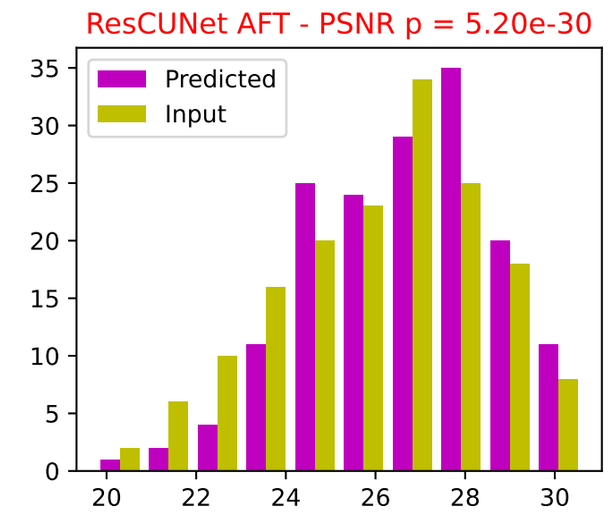

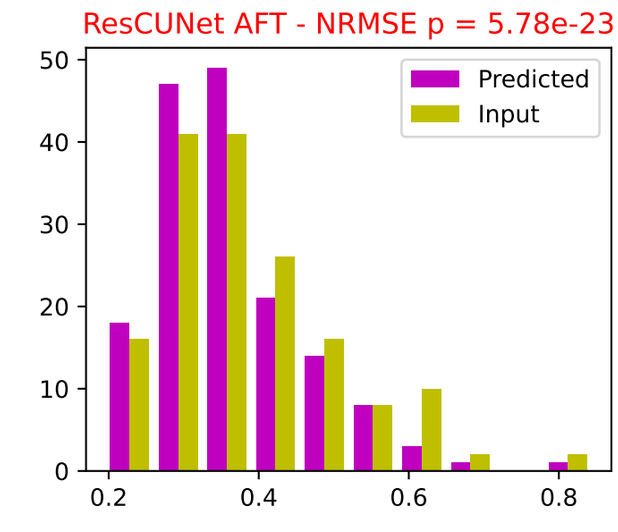

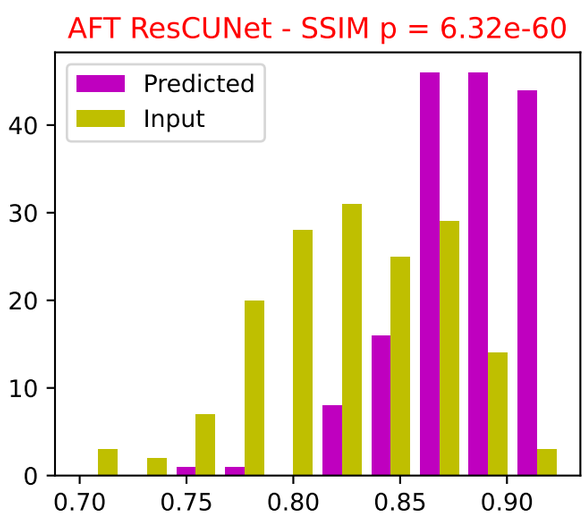

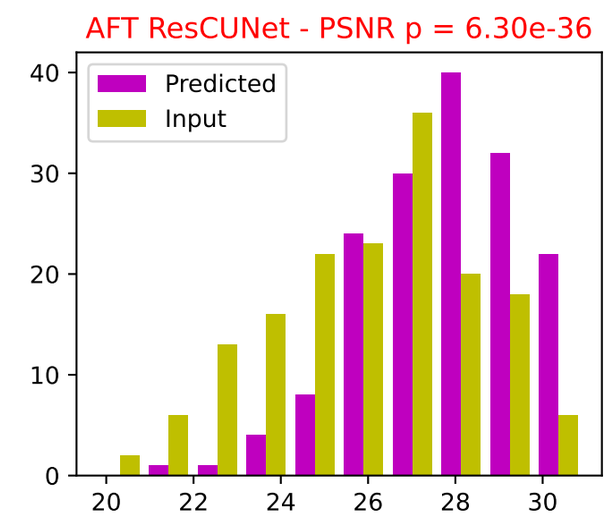

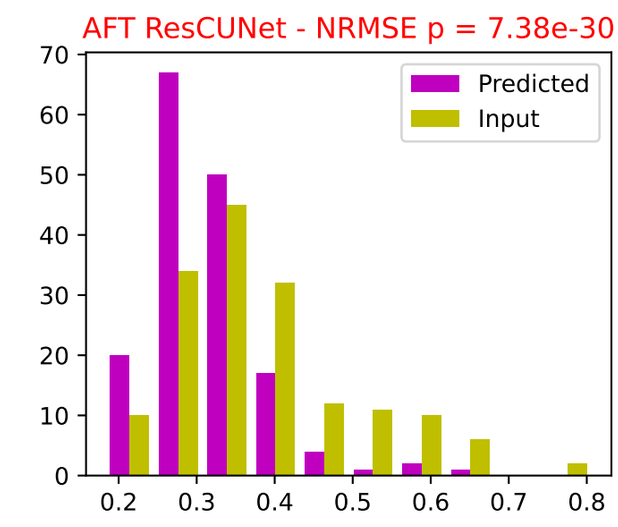

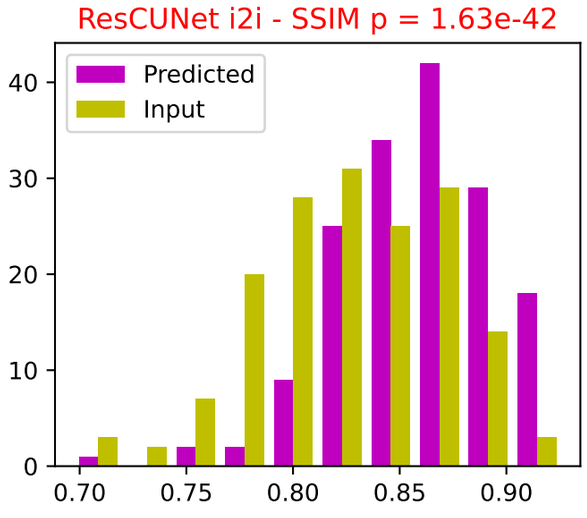

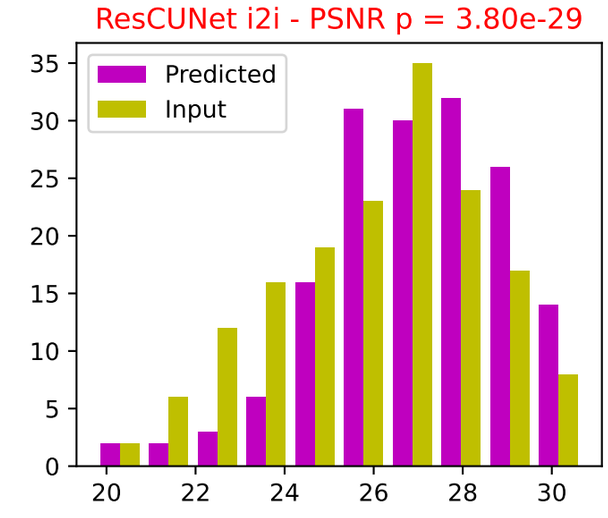

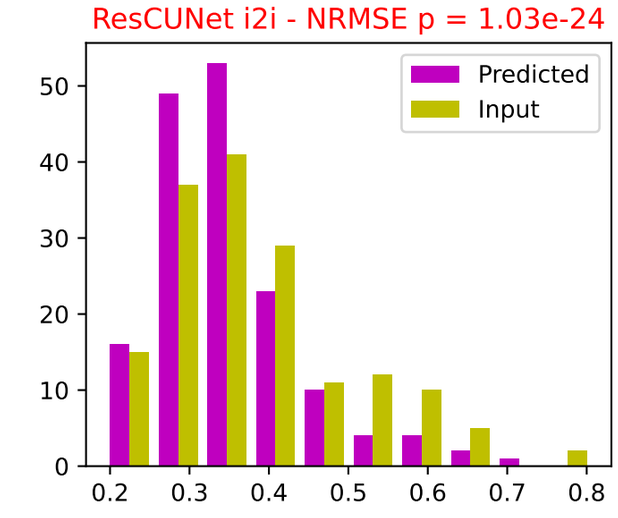

Metric distributions: T1 3T Corrupted

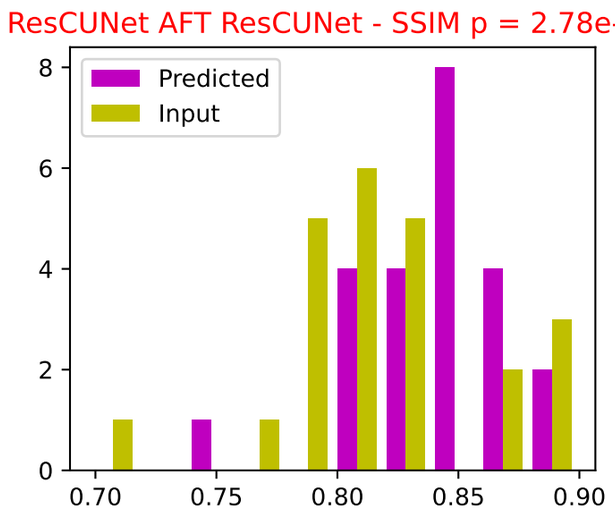

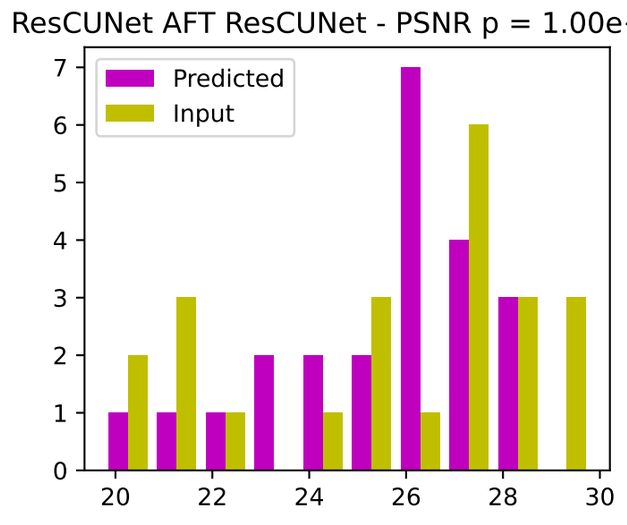

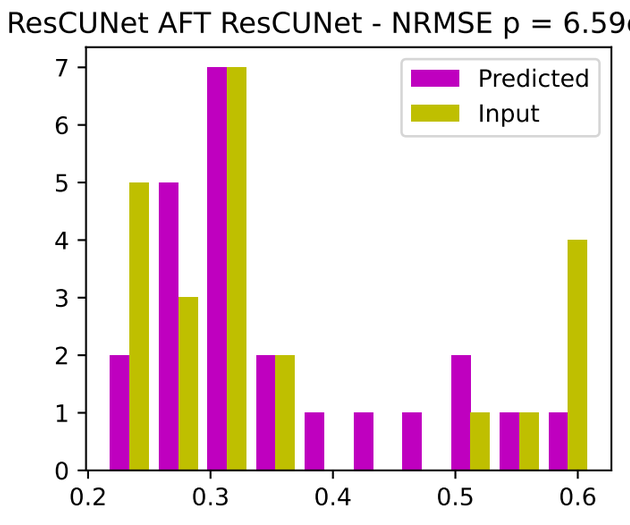

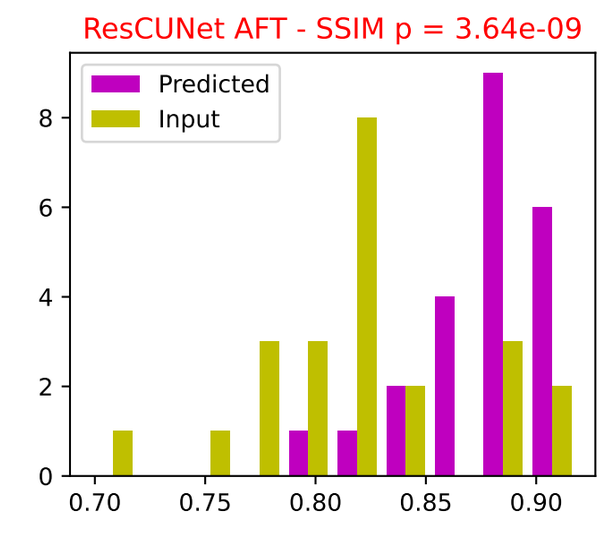

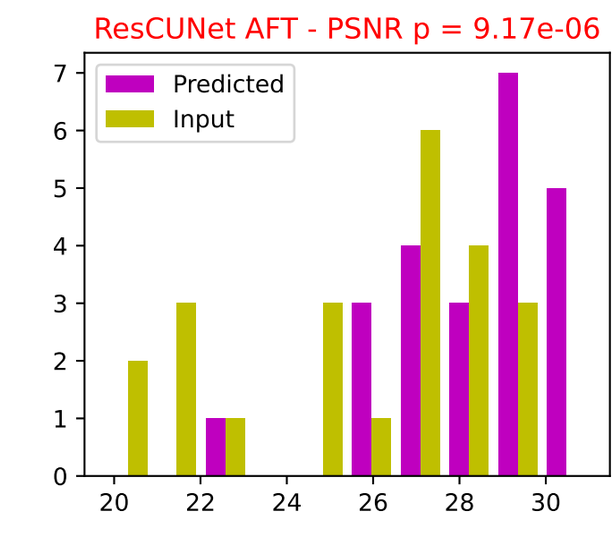

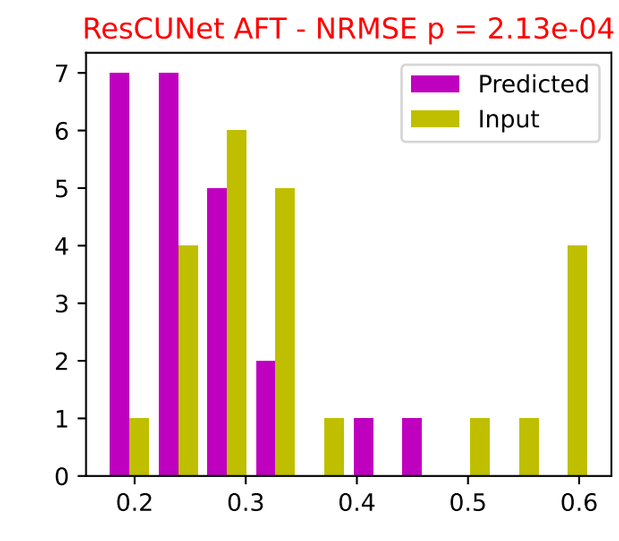

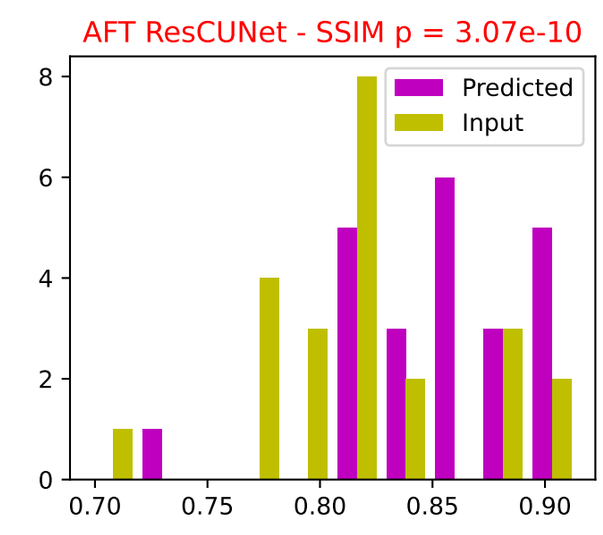

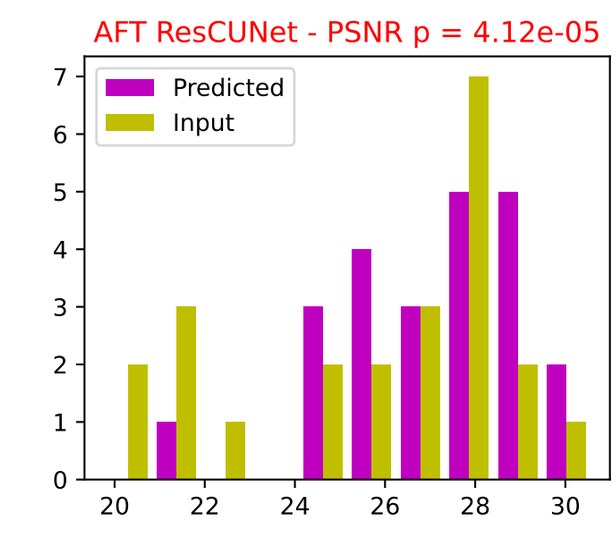

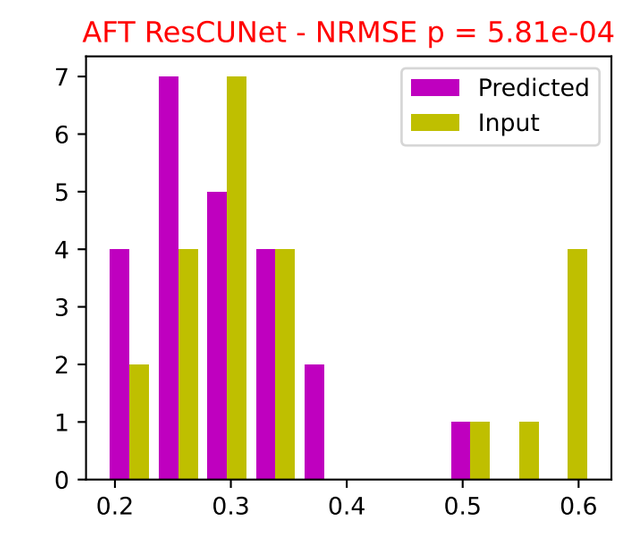

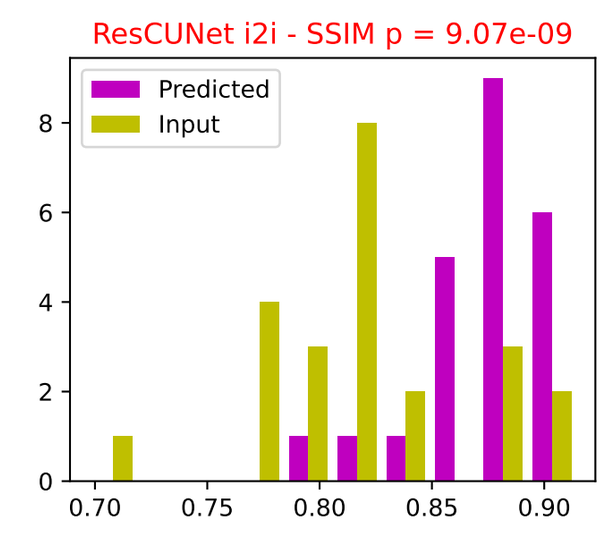

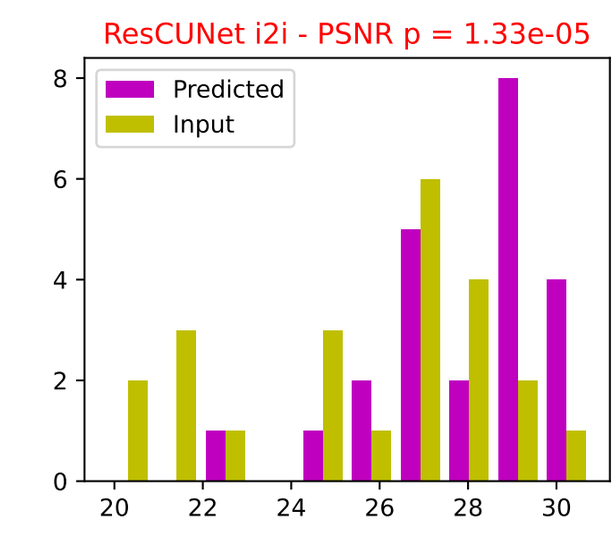

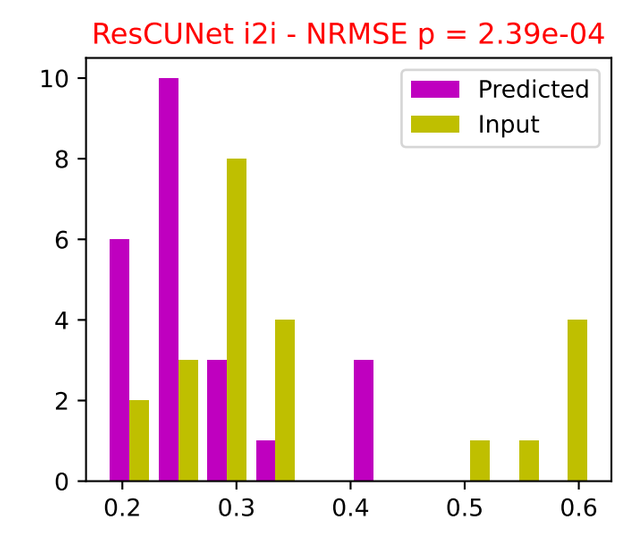

Metric distributions: T2 15T Corrupted

ResCUNet AFT ResCUNet - SSIM p = 4.32e-42

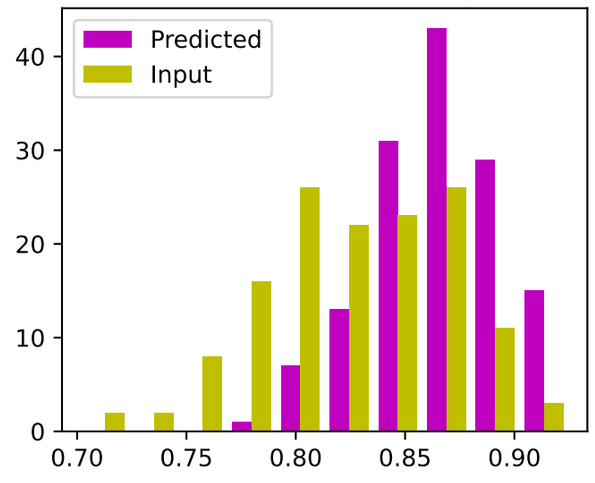

ResCUNet AFT ResCUNet - PSNR p = 3.24e-27

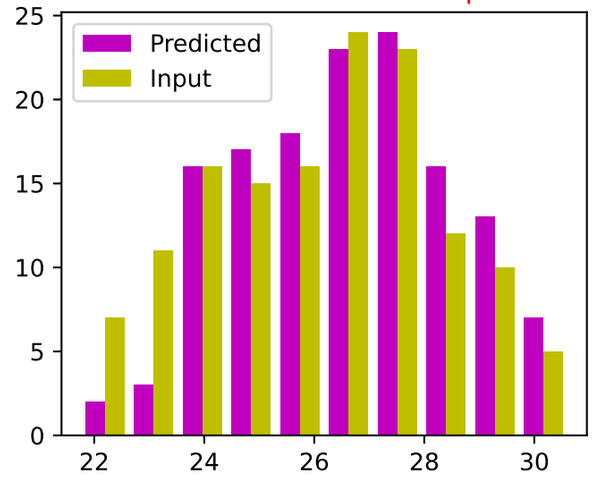

ResCUNet AFT ResCUNet - NRMSE p = 9.31e-20

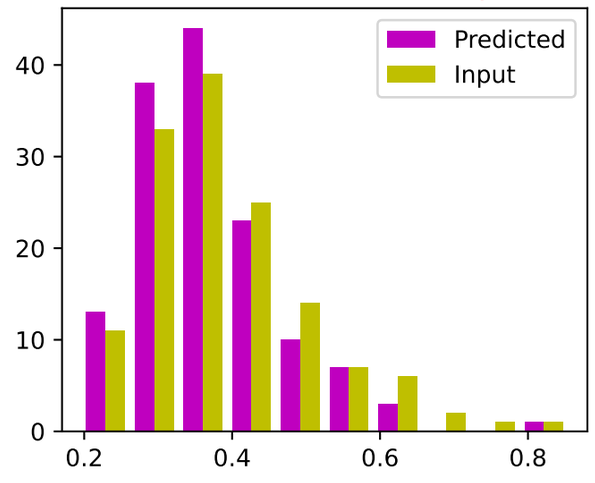

ResCUNet AFT - SSIM p = 9.55e-52

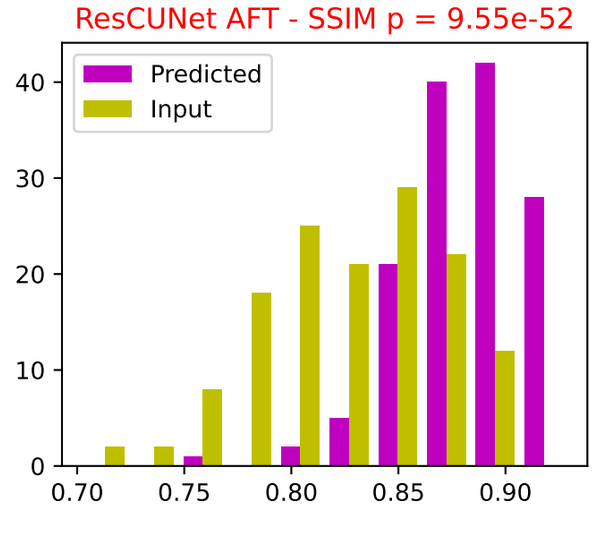

ResCUNet AFT - PSNR p = 6.08e-29

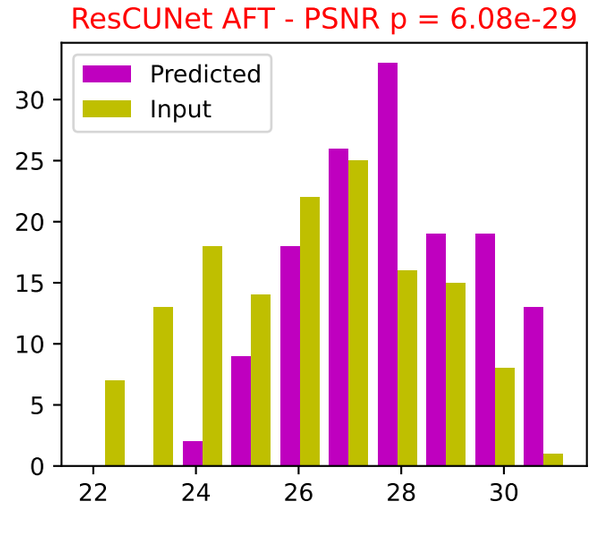

ResCUNet AFT - NRMSE p = 3.30e-25

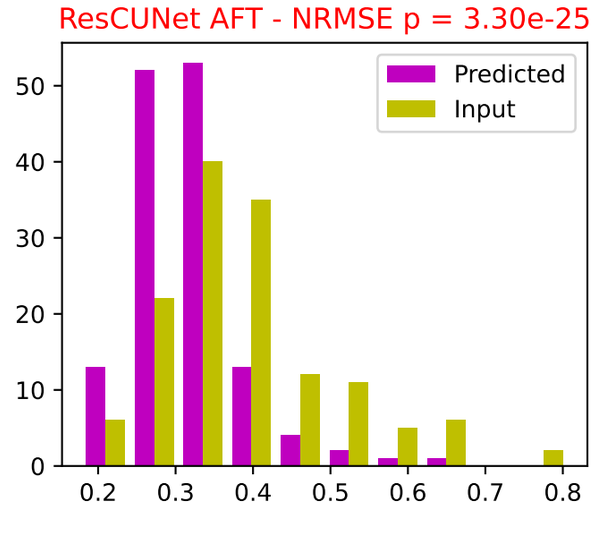

AFT ResCUNet - SSIM p = 1.28e-52

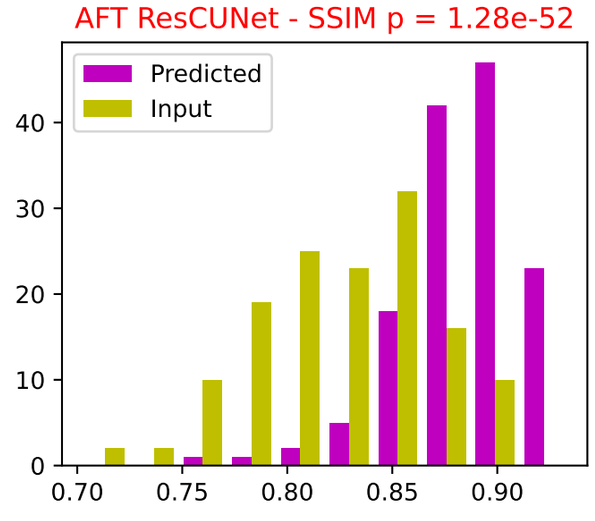

AFT ResCUNet - PSNR p = 1.42e-32

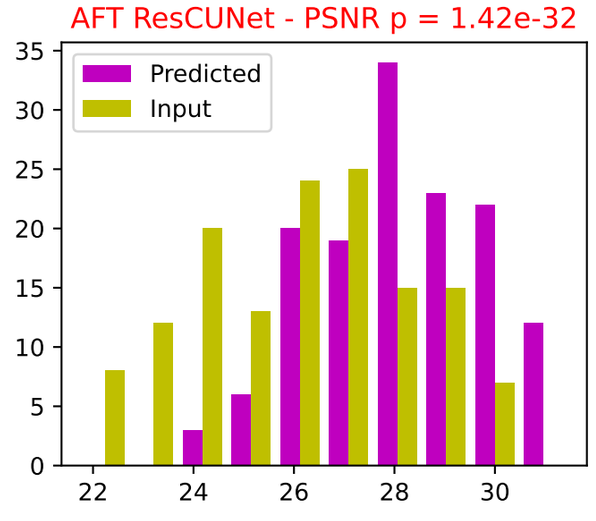

AFT ResCUNet - NRMSE p = 5.73e-27

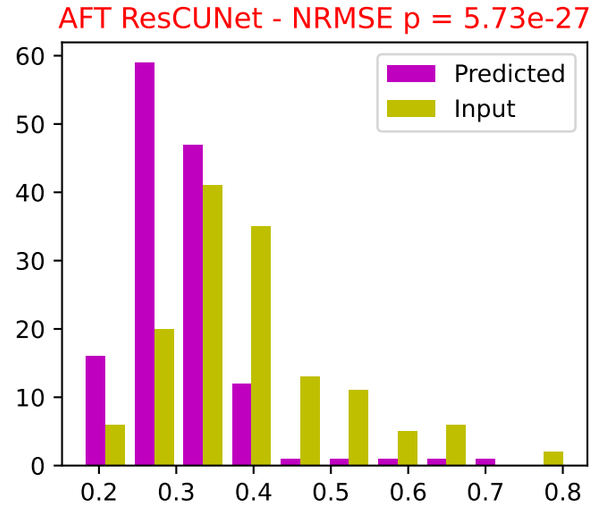

ResCUNet i2i - SSIM p = 1.31e-48

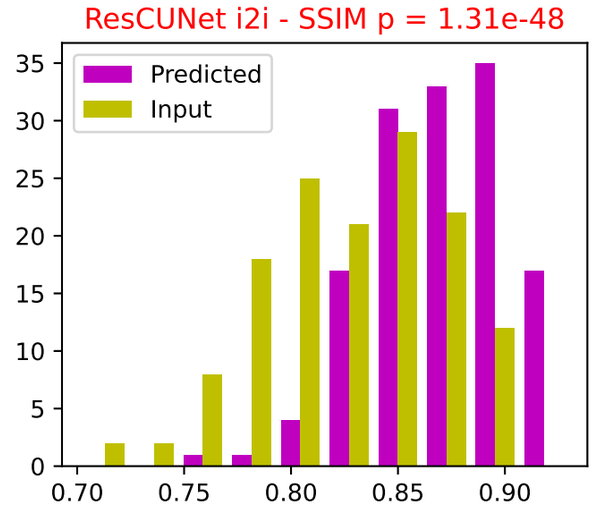

ResCUNet i2i - PSNR p = 1.82e-26

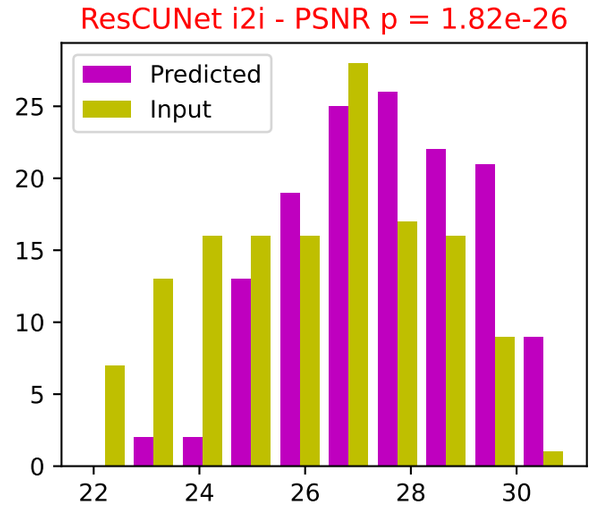
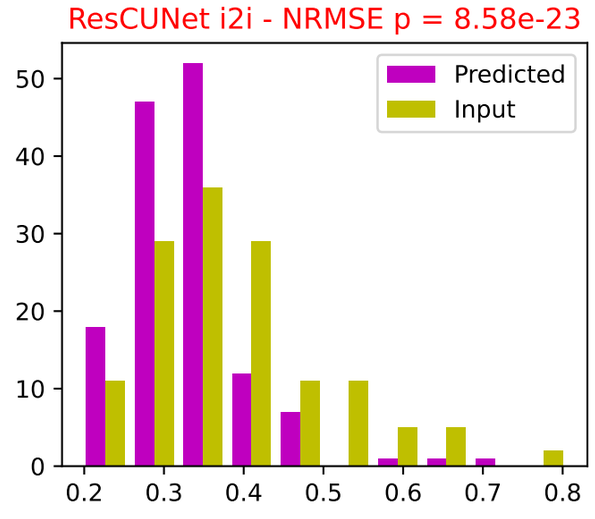
ResCUNet i2i - NRMSE p = 8.58e-23